Polar Solvation Dynamics in the Femtosecond Evolution of Two-Dimensional Fourier Transform Spectra

John D. Hybl,† Anchi Yu, Darcie A. Farrow, and David M. Jonas*

Department of Chemistry and Biochemistry, University of Colorado, Boulder, Colorado 80309-0215

Received: April 30, 2002; In Final Form: July 9, 2002

Femtosecond two-dimensional Fourier transform (2D FT) spectra remove inhomogeneity and simultaneously provide time resolution and two dimensions (excitation, signal) of frequency resolution limited only by the sample. The time evolution of separate real and imaginary 2D FT spectra is used to study local environments around molecules in methanol. Polar solvation dynamics are extracted by comparing 2D FT spectra of structurally related dyes with and without spectral sensitivity to solvent polarity. This comparison reveals specific signatures of inertial motion and the dynamic Stokes' shift.

The spectra of molecules in solution are usually featureless because of strong interactions with the solvent. Solute interactions with polar solvents can control charge transfer reactions by differentially stabilizing reactants, products, and the fleeting intermediate transition state. The dynamics of polar solvation are important in determining charge transfer rates because solvent fluctuations are needed to roughly zero the energy gap between reactants and products at the transition state.[1] However, the fast dynamics are hidden under an ensemble average over different local environments in linear absorption spectra, so femtosecond nonlinear spectroscopy has been used in attempts to peer beneath the absorption line shape.[2−4]

Several years ago, molecular dynamics simulations pointed to an energetically dominant "inertial" portion of the polar solvation dynamics with a time scale as fast as ∼100 fs in small polar solvents (faster in water).[5] Inertial solvation is distinguished from the subsequent exponential solvent relaxation because it arises from the effect of preexisting thermal motion on the electronic energy gap. When the solute charge distribution is suddenly changed by optical excitation, the resulting change in force on the solvent causes changes in the evolution of these solvent coordinates which also develop as t^2. This stabilization of the new charge distribution causes a drop in frequency known as the dynamic Stokes' shift.

Although several experiments have shown a solvent response of the expected magnitude and time scale, characterization of polar inertial solvation and the dynamic Stokes' shift has been tricky for two reasons: (1) intramolecular vibrational and nonpolar mechanical responses occur on the same time scale; and (2) the rapid frequency shifts imply that one cannot match a transform limited pulse to a "homogeneous line shape" underneath the "inhomogeneous" spectrum. Comparing similar molecules in the same solvent is a new approach to the first problem. Measuring the time dependent evolution of their two-dimensional Fourier transform (2D FT) spectra solves the second.

Like most cyanine dyes, the spectrum of HDITCP is sensitive only to solvent polarizability and insensitive to orientational solvent polarity (nonpolar solvatochromism). IR144 has the same structure as HDITCP except for the addition of three functional groups which make the spectrum sensitive to solvent polarity.[6] Both molecules are free of excited-state absorption near 800 nm, so comparison of their nonlinear spectra allows differentiation between polar and nonpolar/vibrational responses in the same solvent.

In magnetic resonance, 2D experiments with high excitation and signal frequency resolution use broadband pulses and obtain frequency resolution by Fourier transforming arrays of nonlinear signal fields with respect to time intervals between pulses.[7] A number of femtosecond experiments have measured nonlinear signals as a function of two variables.[4,8−13] The femtosecond evolution of 2D FT spectra in a third time dimension is examined here. In contrast to conventional femtosecond spectroscopy, the time and frequency resolution of 2D FT spectra can reach the minimum uncertainty limit set by molecular dynamics.[14] Real (absorptive) and imaginary (refractive) 2D FT spectra are generated by balancing rephasing and nonrephasing coherence pathways and measuring the nonlinear signal fields at the sample[9,14] (including constant signal phase shifts[15] relative to the excitation pulses).

A cavity dumped titanium sapphire laser generates near Gaussian 22 fs pulses (temporal intensity full width at half-maximum) centered at 12 590 cm^{-1} with a 640 cm^{-1} spectral intensity full width at half-maximum (time bandwidth product 0.43). The signal fields for 2D FT spectra are generated by a noncollinear three-pulse sequence. The first pulse (wave-vector $\vec{k}_a$) sets electronic dipoles oscillating and the second pulse ($\vec{k}_b$) enhances or suppresses these oscillations depending on the dipole frequency, delay τ, and position in the sample. This writes a grating in the sample, with the dipole oscillation frequency stored in the τ dependent grating phase. After a relaxation time T, the third pulse ($\vec{k}_c$) stimulates the grating to radiate a background free signal ($\vec{k}_s = \vec{k}_c + \vec{k}_b - \vec{k}_a$). As in first-order diffraction, the grating phase is transferred to the signal, so the signal is phase modulated by the dipole oscillation during τ. The complete signal field $E_s(t,\tau,T)$ is detected at the sample for a set of τ, and the set is double Fourier transformed with respect to t and τ to make a 2D spectrum with frequencies ω_t and ω_τ.[9] The time delay and phase shift of the signal field relative to the excitation pulses are separately determined (to ±0.02 fs and ±0.05 rad precision, respectively), and delays between excitation

* Corresponding author. Department of Chemistry and Biochemistry, 215 UCB, University of Colorado, Boulder, CO 80309-0215. Tel. (303) 492-3818. Fax (303) 492-5894. E-mail: david.jonas@colorado.edu

† Present address: Lincoln Laboratory, Massachusetts Institute of Technology, L-140A, 244 Wood St., Lexington, MA 02420.

10.1021/jp026047j CCC: $22.00 © 2002 American Chemical Society
Published on Web 08/02/2002

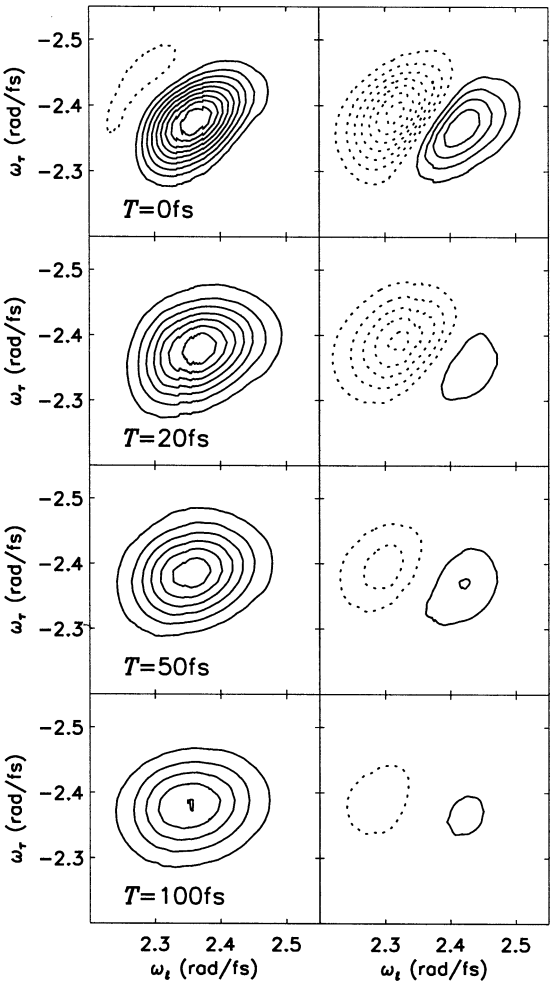

Figure 1. Experimental real (left) and imaginary (right) 2D spectra of IR144 in methanol for four values of T (top to bottom). Contours are drawn at 10% of the $T = 0$ real maximum in both real and imaginary spectra. Positive contours (solid) represent decreased absorption or increased refractive index; negative contours are dashed. The top to bottom sequence of 2D spectra shows the rapid loss of correlation between excitation frequency ω_τ and signal frequency ω_t as the relaxation time T is increased.

pulses are measured to ±0.04 fs.[14] At each T, 601 signal-reference spectral interferograms are recorded over $-200\ \text{fs} \leq \tau \leq 200$ fs. (For negative τ, the pulse with wave-vector $\vec{k}_b$ is first, followed by $\vec{k}_a$.) 2D spectra were measured for 10 values of T from −5 fs to 100 ps.

In 2D FT spectra, the frequency resolution limit is set by the maximum interval between pulses while the time resolution limit is set by the pulse duration.[14] With sufficiently short pulses and long scans, the frequency and time resolution are both set by the sample. For a given excitation pulse $\hat{E}(\omega_t)$, the real parts of the complex 2D spectra are related to pump−probe signals S_{pp} and spectrally resolved pump−probe signals S_{srpp} by integration over frequency[14]

$$S_{srpp}(T,\omega_t) = \text{Re}\left[\frac{\omega_t \hat{E}(\omega_t)^*}{2\pi}\int_{-\infty}^{\infty} d\omega_\tau \hat{S}_{2D}(T,\omega_t,\omega_\tau)\right]$$

$$S_{pp}(T) = \int_{-\infty}^{\infty} d\omega_t S_{srpp}(T,\omega_t)$$

Experimental 2D spectra of IR144 in methanol are shown for four values of T in Figure 1. Positive real 2D amplitude indicates that excitation at ω_τ causes a reduction in absorption at ω_t, proving that the same molecule absorbs or emits both frequencies. The two frequencies have opposite signs because photon echo type rephasing signals have been selected for $\tau > 0$. Similarly, the imaginary 2D spectrum separates the overall refractive index change according to the excitation frequency.

At $T = 0$, the real and imaginary slices of the 2D spectrum for each ω_τ display a near Kramers−Kronig relation with respect to ω_t. For a homogeneously broadened line, the 2D spectrum will be a product of homogeneous line shapes in each frequency dimension. The limitation of real 2D amplitude to a region along the diagonal $\omega_t \simeq -\omega_\tau$ at $T = 0$ suggests inhomogeneous broadening: molecules with different frequencies are spread along the diagonal because 2D spectra are additive. For true inhomogeneous broadening, the cross-width of the 2D spectrum perpendicular to the diagonal is related to the homogeneous line width. However, the negative region above the diagonal directly indicates that the profile perpendicular to the diagonal is not simply a homogeneous line shape (a homogeneous line shape is positive). In two-state systems, computations have shown that negative regions are a signature of frequency memory.[16] Also, the 2D spectrum peaks above the diagonal, not on it. At $T = 0$, such asymmetry arises from correlation between frequency shifts of the coherently oscillating dipoles during τ and t such that $|\omega_\tau| \geq |\omega_t|$ (i.e., a coherent aspect of the dynamic Stokes' shift).[16] Furthermore, the cross-width of the 2D spectrum is narrower than the vibrational width of the IR144 electronic spectrum by over 30% because the femtosecond 2D FT spectrum freezes out rapidly moving vibrational and solvent coordinates as "inhomogeneities". These new aspects of femtosecond 2D spectroscopy, first predicted computationally,[16] are not present in 2D NMR.

The rapid evolution of the 2D spectrum with T reflects the rapid Stokes' shifts caused by both intramolecular vibrations and the surrounding solvent during the population relaxation time T (there is a weak distortion from rephasing/nonrephasing imbalance when all three pulses overlap near $T = 0$[16]). As T is increased, the ground-state hole and excited-state wave packet contributions to the 2D spectrum (which coincide at $T = 0$) evolve toward the equilibrium absorption and emission spectra in the ω_t dimension. (This evolution gradually destroys the correlation between dipole oscillation frequencies during τ and t that causes the asymmetry at $T = 0$.) Since the emission spectrum is at lower energy than the absorption spectrum, the equilibrated 2D spectrum has an excited-state emission contribution centered above the diagonal ($|\omega_\tau| > |\omega_t|$). With excitation pulse spectra centered halfway between the equilibrium absorption and emission spectra, the result is a nearly symmetric spreading. Because the excitation pulse spectra do not cover the entire molecular spectrum, frequency shifts beyond the excitation spectra cause a reduction in real 2D amplitude. Finite bandwidth departures from the 2D Kramers−Kronig relation become prominent as the absorption change spreads outside the pulse spectrum with increasing T. However, the imaginary (refractive) 2D spectrum is sensitive to spectral shifts outside the pulse spectrum (just as the linear refractive index is sensitive to absorption at all frequencies, with nearby frequencies weighted most heavily). The tilt of the nodal line in the imaginary spectrum reflects the evolution of the full real spectrum toward homogeneous broadening as it evolves from diagonal toward vertical.

Three differences between the 2D spectra of IR144 and the nonpolar reference solute HDITCP (see Figure 2) are notable: (1) At every T, the cross-width of the HDITCP spectrum perpendicular to the diagonal is ∼15% narrower; (2) The negative region above the diagonal at $T = 0$ only reaches the

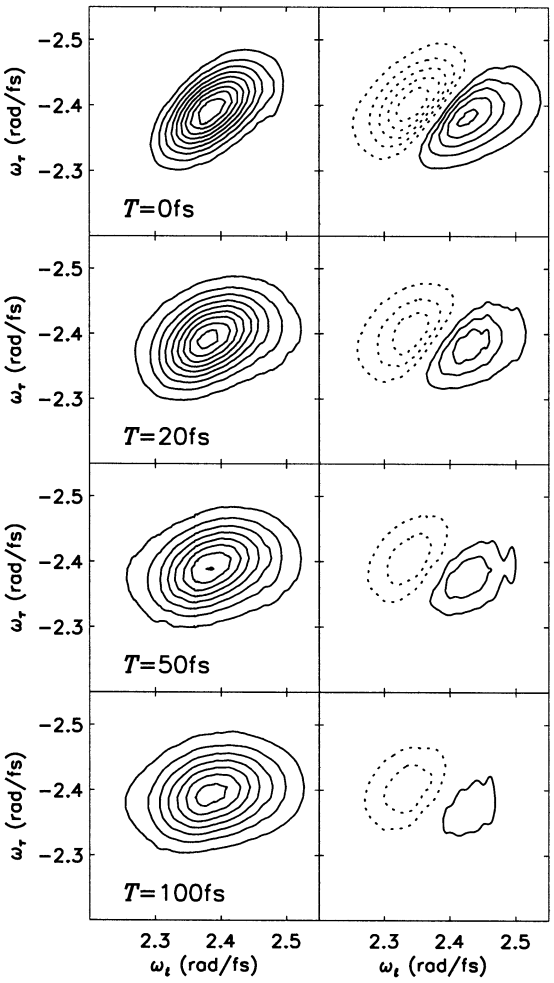

Figure 2. Experimental real (left) and imaginary (right) 2D spectra of HDITCP in methanol for four values of T (top to bottom) for comparison with Figure 1. In contrast to IR144, HDITCP has a nonpolar solute−solvent interaction, so differences are attributed to the polar solvation of IR144.

−7% contour in HDITCP (vs. −17% in IR144); and (3) The loss of real 2D amplitude is slower in HDITCP, only dropping to 75% by $T = 100$ fs (vs. 50% in IR144). Although these dyes do not dissolve in nonpolar solvents, a model attributing these differences to polar solvation is supported by the similarity in structure, difference in solvatochromism,[17] and nearly identical pump−probe vibrational quantum beats.[6]

The Brownian oscillator model is the simplest model for the nonlinear optical response which includes damping, a gradual change of the electronic frequency, and a dynamic Stokes' shift.[18] This model requires a frequency, a displacement upon excitation, and a damping rate for each vibrational or solvent mode and assumes that electronic excitation displaces the equilibrium harmonic oscillator potential for each nuclear coordinate without changing the oscillator frequency. Brownian random forces for the damping ensure thermal equilibration. A zero-order model for IR144 is built on that for HDITCP by adding polar solvation modes. The multimode Brownian oscillator model used for HDITCP extends that developed in ref 19 to reproduce the HDITCP femtosecond 2D spectra, photon echo slices through the nonlinear signal field $E(t = \tau;T)$,[16] pump−probe transients extending to 1.1 ns delay, and the linear spectra. This model was extended to IR144 by adding two overdamped modes to account for picosecond polar solvation dynamics plus a critically damped oscillator to represent inertial solvation. When the polar solvation model was refined to match the IR144

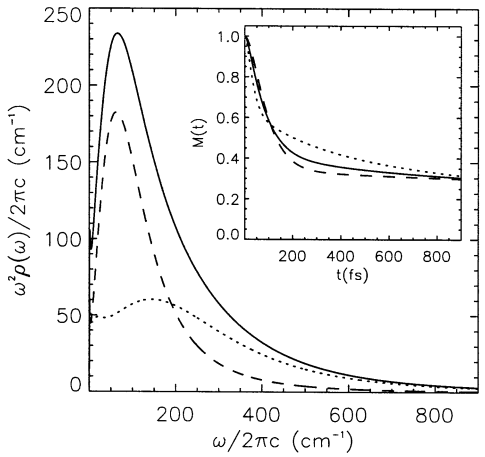

Figure 3. Solvation spectral density from the IR144/methanol Brownian oscillator model. The solid curve is the total IR144 solvation spectral density. The dotted HDITCP spectral density is attributed to a combination of intramolecular relaxation and nonpolar solvation present in both molecules. The dashed curve is the difference between IR144 and HDITCP spectral densities, attributed to polar solvation. Inset: Corresponding solvation frequency−frequency correlation functions.

2D spectra, photon echo slices, and pump−probe transients, it spontaneously yielded good agreement with the IR144 linear absorption spectrum. The fit to the pump−probe transients and photon echo slices extracted from the 2D data is quantitative, but the model cannot capture departures from mirror image symmetry between absorption and emission[6] or some slight distortions of the 2D spectra expected to arise at the 10% level due to propagation inside the sample.[14] However, all of the differences between the 2D spectra of HDITCP and IR144 noted above are reproduced. Since a model with mirror image symmetry is adequate for the first 100 fs, the spontaneous agreement with the IR144 absorption spectrum suggests that the severe departure from mirror image symmetry in IR144 (attributed to pyramidalization of the piperazine nitrogen)[6] develops on a picosecond time scale.

The solvation dynamics can be viewed either in the time domain [as a frequency−frequency correlation function $M(t)$] or the frequency domain [as a corresponding spectral density $\rho(\omega)$] in Figure 3. The high-temperature limit applies for polar solvation, so these are related by

$$M(t) = \frac{\beta}{2\pi\lambda}\int_0^\infty \omega^2\rho(\omega)\coth(\beta\hbar\omega/2)\cos(\omega t)\,\mathrm{d}\omega$$

where λ is the reorganization energy and $\beta = 1/k_B T$ is the inverse temperature. Because the Brownian oscillator modes may effectively represent either many processes or a single complex relaxation, a weighted total solvation correlation function and spectral density are used. In the time domain, inertial solvation causes the frequency−frequency correlation function to decay by 60% within 200 fs, followed by picosecond biexponential decay. All three of these decays are faster for HDITCP (nonpolar solute−solvent interaction) than IR144 (polar solute−solvent interaction). The inertial decay is in reasonable agreement with molecular dynamics simulations,[20,21] and faster than the time resolution of upconversion experiments.[22]

Unresolved high frequency vibrations[4] account for one third of the solvent spectral density previously reported for IR144.[2] A fast, weakly solvent dependent dephasing observed in HDITCP accounts for another quarter (this response includes both intramolecular and intermolecular overdamped motions). The remaining polar solvation spectral density, which peaks at

around 95 cm^{-1}, is dominated by the inertial response in $M(t)$ and accounts for the solvent polarity dependent "coherence spike" seen in pump−probe transients of IR144 but not of HDITCP. This polar solvation spectral density change is more accurately attributed to solute−solvent interaction than either total spectral density because common intramolecular responses cancel. It should be emphasized that Figure 3 shows the change in the low frequency spectral density caused by polar solvation and does not imply a physical separation of polar and nonpolar solvation processes, which may be strongly coupled.[23]

Despite sufficient time resolution, the spectral densities in Figure 3 show no obvious sign of OH libration near 600 cm^{-1}. The polar solvation spectral density change peaks at lower frequencies than the corresponding spectral densities derived from the polarizability anisotropy (154 cm^{-1})[24] or the infrared spectrum of pure methanol (∼130 cm^{-1}). These broad peaks extending to zero frequency have been associated with rotational motions about axes roughly perpendicular to the CO bond.[20] Since the charge rearrangement upon electronic excitation of IR144 redistributes partial positive charges on nitrogen atoms,[6] motion of O atoms caused by rotations about CO bonds might be expected to play a larger role than motion of H atoms caused by high frequency OH librations. Thus, a solvation spectral density within this broad CO rotation peak seems reasonable and is supported by a variety of simulations. The frequencies may be lower near the shifting charges in IR144 than in pure methanol, or even lower frequency intermolecular modes involving methanol translation[25] may play a role.

In addition to revealing polar solvation dynamics of methanol, the separate real and imaginary 2D FT spectra highlight important differences between optical 2D spectra and their NMR counterparts. Because femtosecond 2D FT spectra "freeze" molecular motion and separate the experimental time and frequency resolution limits, they provide a new route to spectroscopy with the shortest available pulses in the optical and infrared regions of the spectrum. The ability to separate the spectra of different chromophores according to instantaneous frequency with uncertainty limited resolution is expected to be valuable for study of dynamics in fluctuating disordered systems.

Acknowledgment. This work was supported by the National Science Foundation, the David and Lucile Packard Foundation, and the Sloan Foundation.

Supporting Information Available: Complete model parameters and simulated 2D spectra of HDITCP and IR144. This material is available free of charge via the Internet at http://pubs.acs.org.

References and Notes

(1) Rossky, P. J.; Simon, J. D. *Nature* **1994**, *370*, 263−269.
(2) Passino, S. A.; Nagasawa, Y.; Fleming, G. R. *J. Chem. Phys.* **1997**, *107*, 6094−6108.
(3) de Boeij, W. P.; Pshenichnikov, M. S.; Wiersma, D. A. *Chem. Phys.* **1998**, *233*, 287−309.
(4) Book, L. D.; Scherer, N. F. *J. Chem. Phys.* **1999**, *111*, 792−795.
(5) Carter, E. A.; Hynes, J. T. *J. Chem. Phys.* **1991**, *94*, 5961−5979.
(6) Yu, A.; Tolbert, C. A.; Farrow, D. A., Jonas, D. M. *J. Phys. Chem. A*, accepted.
(7) Ernst, R. R.; Bodenhausen, G.; Wokaun, A. *Principles of nuclear magnetic resonance in one and two dimensions*; Oxford University Press: Oxford, 1987.
(8) Lepetit, L.; Joffre, M. *Opt. Lett.* **1996**, *21*, 564−566.
(9) Hybl, J. D.; Albrecht, A. W.; Gallagher Faeder, S. M.; Jonas, D. M. *Chem. Phys. Lett.* **1998**, *297*, 307−313.
(10) Mukamel, S. *Annu. Rev. Phys. Chem.* **2000**, *51*, 691−729.
(11) Asplund, M. C.; Zanni, M. T.; Hochstrasser, R. M. *Proc. Natl. Acad. Sci. U.S.A.* **2000**, *97*, 8219−8224.
(12) Merchant, K. A.; Thompson, D. E.; Fayer, M. D. *Phys. Rev. Lett.* **2001**, *86*, 3899−3902.
(13) Golonzka, O.; Khalil, M.; Demirdöven, N.; Tokmakoff, A. *Phys. Rev. Lett.* **2001**, *86*, 2154−2157.
(14) Hybl, J. D.; Albrecht Ferro, A.; Jonas, D. M. *J. Chem. Phys.* **2001**, *115*, 6606−6622.
(15) Xu, L.; Spielmann, C.; Poppe, A.; Brabec, T.; Krausz, F.; Hänsch, T. W. *Opt. Lett.* **1996**, *21*, 2008−2010.
(16) Hybl, J. D.; Christophe, Y.; Jonas, D. M. *Chem. Phys.* **2001**, *266*, 295−309.
(17) Reichardt, C., *Solvents and Solvent Effects in Organic Chemistry*, 2nd ed.; VCH: Verlagsgesellschaft, Germany, 1988.
(18) Mukamel, S. *Principles of Nonlinear Optical Spectroscopy*; Oxford University Press: New York, 1995.
(19) Yang, T.-S.; Chang, M.-S.; Chang, R.; Hayashi, M.; Lin, S. H.; Vöhringer, P.; Dietz, W.; Scherer, N. F. *J. Chem. Phys.* **1999**, *110*, 12070−12081.
(20) Ladanyi, B. M.; Skaf, M. S. *Annu. Rev. Phys. Chem.* **1993**, *44*, 335−368.
(21) Kumar, P. V.; Maroncelli, M. *J. Chem. Phys.* **1995**, *103*, 3038−3060.
(22) Horng, M. L.; Gardecki, J. A.; Papazyan, A.; Maroncelli, M. *J. Phys. Chem.* **1995**, *99*, 17311−17337.
(23) Aherne, D.; Tran, V.; Schwartz, B. J. *J. Phys. Chem. B* **2000**, *104*, 5382−5394.
(24) Shirota, H.; Yoshihara, K.; Smith, N. A.; Lin, S.; Meech, S. R. *Chem. Phys. Lett.* **1997**, *281*, 27−34.
(25) Ladanyi, B. M.; Stratt, R. M. *J. Phys. Chem.* **1995**, *99*, 2502−2511.